Geomechanics and Engineering, *Vol. 14, No. 2 (2018) 161-174*
DOI: https://doi.org/10.12989/gae.2018.14.2.161

SSI effects on seismic behavior of smart base-isolated structures

Saeed Shourestani[1a], Fazlollah Soltani[1b], Mojtaba Ghasemi[1b] and Sadegh Etedali[*2]

[1]*Department of Civil and Surveying Engineering, Graduate University of Advanced Technology, Kerman, Iran*
[2]*Department of Civil Engineering, Birjand University of Technology, Birjand, Iran*

(Received January 3, 2017, Revised June 22, 2017, Accepted July 8, 2017)

Abstract. The present study investigates the soil-structure interaction (SSI) effects on the seismic performance of smart base-isolated structures. The adopted control algorithm for tuning the control force plays a key role in successful implementation of such structures; however, in most studied carried out in the literature, these algorithms are designed without considering the SSI effect. Considering the SSI effects, a linear quadratic regulator (LQR) controller is employed to seismic control of a smart base-isolated structure. A particle swarm optimization (PSO) algorithm is used to tune the gain matrix of the controller in both cases without and with SSI effects. In order to conduct a parametric study, three types of soil, three well-known earthquakes and a vast range of period of the superstructure are considered for assessment the SSI effects on seismic control process of the smart-base isolated structure. The adopted controller is able to make a significant reduction in base displacement. However, any attempt to decrease the maximum base displacement results in slight increasing in superstructure accelerations. The maximum and RMS base displacements of the smart base-isolated structures in the case of considering SSI effects are more than the corresponding responses in the case of ignoring SSI effects. Overall, it is also observed that the maximum and RMS base displacements of the structure are increased by increasing the natural period of the superstructure. Furthermore, it can be concluded that the maximum and RMS superstructure accelerations are significant influenced by the frequency content of earthquake excitations and the natural frequency of the superstructure. The results show that the design of the controller is very influenced by the SSI effects. In addition, the simulation results demonstrate that the ignoring the SSI effect provides an unfavorable control system, which may lead to decline in the seismic performance of the smart-base isolated structure including the SSI effects.

Keywords: base isolation; soil-structure interaction; smart base-isolated structures; LQR controller; particle swarm optimization algorithm

1. Introduction

Seismic isolation is an innovative technology to improve seismic performance and to minimize vulnerability of buildings and bridges during earthquakes and strong winds (Etedali and Sohrabi 2016). SSI effects modify the characteristics of structures such as natural frequencies, damping ratios and shape mode (Wolf 1989). SSI effects could play a significant role on seismic performance of structures. However, seismic behavior of such structures is often studied based on the rigid base assumption without considering SSI effects. Seismic behavior of base-isolated structures by taking into account the SSI effects has been studied by several researchers during the last few years. Most studies considered the SSI effects on base isolated bridges and liquid storage tanks (Chaudhary *et al.* 2001, Vlassis and Spyrakos 2001, Spyrakos and Vlassis 2002, Iemura and Pradono 2002, Kim *et al.* 2002, Tongaonkar and Jangid 2003, Cho *et al.* 2004, Sarrazin *et al.* 2005, Kunde and Jangid 2006, Soneji and Jangid 2008). However, few studies have been carried out on the response of isolated buildings with SSI effects. Constantinou and Kneifati (1986) have studied the SSI effects on dynamic characteristics of base-isolated structures. They also examined the ability of a simple energy-based method to achieve satisfying and appropriate results. Numerical analysis carried out by Tsai *et al.* (2004) on friction pendulum isolators have demonstrated that SSI effects lead to a larger displacement and in some parts of the structures lead to greater shear forces. The SSI effects on damping, frequency and mass ratios of an isolated building modelled as a SDOF system are investigated by Spyrakos *et al.* (2009). Also, they derived a series of analytical expressions in the frequency domain to investigate the SSI effect on base- isolated building subjected to harmonic ground motions (Spyrakos *et al.* 2009). Mahmoud *et al.* (2012a) conducted modeling of base-isolated buildings considering soil flexibility toward seismic response time history analyses. They also investigated seismic behavior of non-linear base isolated building considering SSI effects (Mahmoud *et al.* 2012b). A numerical procedure to compute the seismic fragility of a base-isolated structure, which is applicable to nuclear power plant components and buildings, is developed by Perotti *et al.* (2013).

Very large displacement of the isolators during near-field earthquakes is a major concern in designing base-isolated buildings (Etedali *et al.* 2013). This issue has led designers to increase size of isolation devices to eliminate the risks of buckling and dislocation of the rubbers of

∗Corresponding author, Assistant Professor
E-mail: etedali@birjandut.ac.ir
[a]M.Sc. Student
[b]Assistant Professor

ISSN: 2005-307X (Print), 2092-6219 (Online)

isolators. Furthermore, it may require large seismic gaps between buildings or large bridge expansion joints. These requirements increase cost of the construction and keeps designers away from the primary goal of seismic isolation which is an economical design (Etedali and Sohrabi 2011). In order to enhance the performance and safety of the base-isolated structures during near-field earthquake excitations, the use of passive, semi-active and active devices has been suggested (Etedali *et al.* 2016). Passive devices can reduce the large deformations of the isolation bearings during strong earthquakes at the cost of significant increase of both internal deformations and absolute accelerations of the superstructure floors. Therefore, many advantages of the isolators are limited. Equipping of base-isolated structures with active and semi-active control systems is one of the most interesting and innovative solutions to get out of this issue. This kind of isolation structure is called a smart isolated structure (Nagarajaiah and Narasimhan 2006). Recently, many studies are carried out to enhance the performance of smart base-isolated building in both near-field and far-field earthquakes (Ozbulut and Hurlebaus 2010, Ozbulut *et al.* 2011, Etedali *et al.* 2013, Zhao and Li 2015, Zamani *et al.* 2016). These studies are carried out based on the rigid base assumption without considering SSI effects, but no study has attempted to investigate the effects of SSI on the smart base-isolated buildings.

The seismic behavior of smart base-isolated structures is significantly affected by the soil-structure interaction. In other words, the process of controller design is based on identification of structural system. The SSI effects significantly modify the dynamic characteristics of structures such as natural frequencies, damping ratios and mode shapes. Ignoring these effects on the design of controller may lead the performance of controller toward deterioration. Hence, this study evaluates the effects of SSI in seismic control process of smart base-isolated structures. Linear quadratic regulator controller is applied to control of the structure. The gain matrix of the controller is tuned using a PSO algorithm in both cases without and with considering SSI effects. In order to carry out a parametric study, three types of soil, three well-known earthquakes and a vast range of period of the superstructure are considered for assessment the SSI effects on seismic control process of a smart-base isolated structure.

The rest of the paper is organized as follows. The mathematical model of a base-isolated structure and smart base-isolated structure with and without SSI effects are introduced in Section 2. A base isolated structure is considered in Section 3 for numerical studied. A vase range numerical studies are also carried out on the structure in this section. Simulation results are discussed in Section 4. The concluding remarks are summarized in Section 5.

2. Mathematical models

2.1 Modeling of a base-isolated structures

A one-degree-of-freedom linear structure subjected to excitation acceleration, $\ddot{u}_g(t)$, is assumed. Considering an isolation system, only the degree-of-freedom of the main structure is added by one. The equation of motion of a base-isolated structure can be written as

$$\boldsymbol{M}\ddot{\boldsymbol{u}}(t) + \boldsymbol{C}\dot{\boldsymbol{u}}(t) + \boldsymbol{K}\boldsymbol{u}(t) + \boldsymbol{F_b}(t) = -\boldsymbol{M}\boldsymbol{R}\ddot{u}_g(t) \quad (1)$$

where $\boldsymbol{M}$, $\boldsymbol{C}$ and $\boldsymbol{K}$ are the mass, damping and stiffness matrices, respectively. If the effects of soil-structure interaction are ignored, they are defined as follows

$$\boldsymbol{M} = \begin{bmatrix} m_s & 0 \\ 0 & m_b \end{bmatrix} \quad \boldsymbol{C} = \begin{bmatrix} c_s & -c_s \\ -c_s & c_b + c_s \end{bmatrix} \quad \boldsymbol{K} = \begin{bmatrix} k_s & -k_s \\ -k_s & k_b + k_s \end{bmatrix} \quad (2)$$

in which m_s, c_s and k_s are mass, damping and stiffness of superstructure, respectively. Also, m_b, c_b and k_b are mass, damping and stiffness of isolation system, respectively. In this case, vectors $\boldsymbol{u}(t)$, $\dot{\boldsymbol{u}}(t)$ and $\ddot{\boldsymbol{u}}(t)$ refer to displacement, velocity and acceleration vectors of the structures, respectively. Furthermore, **R** is location vector for an earthquake and $\mathbf{F_b}(t)$ denotes the restoring force vector of the isolator. These vectors can be given as

$$\boldsymbol{R} = \begin{bmatrix} 1 \\ 1 \end{bmatrix} \quad \boldsymbol{u}(t) = \begin{bmatrix} u_s(t) \\ u_b(t) \end{bmatrix} \quad \boldsymbol{F_b}(t) = \begin{bmatrix} 0 \\ f_b(t) \end{bmatrix} \quad (3)$$

in which $u_s(t)$ and $u_b(t)$ are the displacement of the superstructure and the base story, respectively. Also, the restoring force of seismic isolation can be obtained as $f_b(t) = k_b u_b(t) + c_b \dot{u}_b(t)$.

2.2 Modeling of a base-isolated structure considering SSI effects

If the effects of the soil-structure interaction are considered in the modeling, as shown in Fig. 1, two degrees of freedom $u_0(t)$ and $\varphi(t)$, which respectively represent the displacement and rotation of the foundation, will be added to the structures. In this case, the matrices **M**, **C** and **K** and the vectors **R**, $\boldsymbol{u}(t)$ and $\boldsymbol{F_b}(t)$ can be expressed as the following form

$$\boldsymbol{M} = \begin{bmatrix} m_b & 0 & m_b & 0 \\ 0 & m_s & m_s & m_s h \\ m_b & m_s & m_0 + m_s + m_b & m_s h \\ 0 & m_s h & m_s h & I_{R0} + m_s h^2 + I_{Rb} + I_{Rs} \end{bmatrix}$$
$$\boldsymbol{C} = \begin{bmatrix} c_s & -c_s & 0 & 0 \\ -c_s & c_b + c_s & 0 & 0 \\ 0 & 0 & c_h & 0 \\ 0 & 0 & 0 & c_r \end{bmatrix} \quad \boldsymbol{K} = \begin{bmatrix} k_s & -k_s & 0 & 0 \\ -k_s & k_b + k_s & 0 & 0 \\ 0 & 0 & k_h & 0 \\ 0 & 0 & 0 & k_r \end{bmatrix} \quad (4)$$

$$\boldsymbol{R} = \begin{bmatrix} 1 \\ 0 \\ 0 \\ 1/h \end{bmatrix} \quad \boldsymbol{u}(t) = \begin{bmatrix} u_s(t) \\ u_b(t) \\ u_0(t) \\ \varphi(t) \end{bmatrix} \quad \boldsymbol{F_b}(t) = \begin{bmatrix} 0 \\ f_b(t) \\ 0 \\ 0 \end{bmatrix} \quad (5)$$

where h, m_0, I_{R0} and I_{Rs} and I_{Rb} m_0, I_{R0} and I_{Rs} and I_{Rb} respectively represent height of superstructure, foundation mass, mass moment of inertia of the foundation, superstructure and base story. A rigid circular foundation on the ground surface is adopted in this study. The structure is supported by this foundation with the swaying and the rocking dashpots, and the corresponding springs. The damping values of the rocking and swaying and dashpots are represented as C_h and C_r, and the stiffness of corresponding springs are indicated as K_h and K_r, respectively. The stiffness of swaying and rocking springs and the damping coefficients of dashpots have been

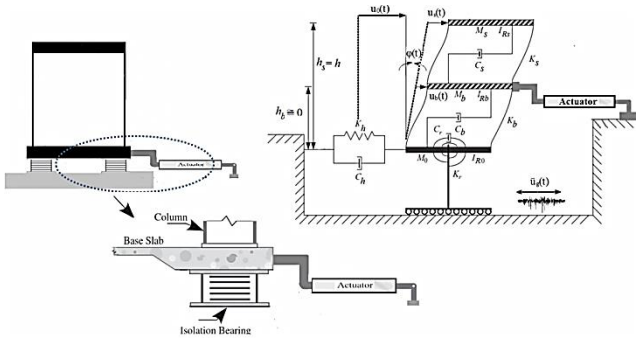

Fig. 1 The idealized mathematical model of base-isolated structures considering SSI effects

evaluated using the formula given by the following equations (Spyrakos *et al.* 2009)

$$k_h = \frac{8Gr}{2-\upsilon} \tag{6}$$

$$c_h = \frac{4.6r^2}{2-\upsilon}\rho V_s \tag{7}$$

$$k_r = \frac{8Gr^3}{3(1-\upsilon)} \tag{8}$$

$$c_r = \frac{0.4r^4}{1-\upsilon}\rho V_s \tag{9}$$

where V_s, υ, ρ, G and r represent the shear wave velocity, Poisson's ratio, density, shear modulus of the soils and the radius of the foundation, respectively.

2.3 Modeling of a smart base-isolated structure considering SSI effects

The equation of motion of a smart base-isolated structure can be given by

$$\boldsymbol{M\ddot{u}}(t) + \boldsymbol{C\dot{u}}(t) + \boldsymbol{Ku}(t) + \boldsymbol{F_b}(t) = -\boldsymbol{MR}\ddot{u}_g(t) + \boldsymbol{D}f(t) \tag{10}$$

where $f(t)$ is the control force and **D** is the location vector of the control force. If the control force is applied to the base story of the structure and the effects of SSI are ignored, **D** is defined as follows

$$\boldsymbol{D} = [0\ 1]^T \tag{11}$$

In this case, the matrices **M**, **C** and **K** and the vectors **R**, $\boldsymbol{u}(t)$ and $\boldsymbol{F_b}(t)$ can be given by Eqs. (2) and (3). Considering the effects of soil-structure interaction, **D** can be obtained as follows

$$\boldsymbol{D} = [0\ 1\ 0\ 0]^T \tag{12}$$

In this case, the matrices **M**, **C** and **K** and the vectors **R**, $\boldsymbol{u}(t)$ and $\boldsymbol{F_b}(t)$ can be given by Eqs. (4) and (5), respectively.

Linear optimal control theory is developed for first-order dynamic systems. In order to apply this theory for seismic control of structures, the second-order motion equation, described in Eq. (10), can be casted into its first-order state-variable representation by defining the following state-vector

$$\boldsymbol{z}(t) = \begin{Bmatrix} \boldsymbol{u}(t) \\ \boldsymbol{\dot{u}}(t) \end{Bmatrix} \tag{13}$$

Considering the above state-vector, Eq. (10) can be rewritten into the state space form as

$$\boldsymbol{\dot{z}}(t) = \boldsymbol{Az}(t) + \boldsymbol{Bf}(t) + \boldsymbol{H}\ddot{u}_g(t) \tag{14}$$

where the state matrix **A**, input matrix **B** and location vector of external excitation **H** are expressed as follows

$$[\boldsymbol{A}] = \begin{bmatrix} \boldsymbol{0} & \boldsymbol{I} \\ -\boldsymbol{M^{-1}K} & -\boldsymbol{M^{-1}C} \end{bmatrix} \qquad [\boldsymbol{B}] = \begin{bmatrix} \boldsymbol{0} \\ \boldsymbol{M^{-1}D} \end{bmatrix} \quad \boldsymbol{H} = \begin{bmatrix} \boldsymbol{0} \\ \boldsymbol{R} \end{bmatrix} \tag{15}$$

where I and 0 respectively represent the identity and zero matrices.

3. Numerical studies

To conduct a parametric study on the seismic performance of smart base-isolated structures, including soil-structure interaction (SSI) effect, a structure equipped with lead rubber bearing (LRB) isolation system in the base story is considered. The mass, damping ratio and the height of the story is adopted as $m_s = 3 \times 10^4$ kg, $\xi_s = 0.05$, and $h = 3.5$ m. For the isolation system, the natural period and the viscous damping ratio of the LRB system are $T_b = 2$ s and $\xi_b = 0.1$, respectively. The base mass is $m_b = 90 \times 10^3$ kg. Furthermore, foundation mass, mass moment of inertia of the foundation, base story and top floor are considered as $m_0 = 1.2 \times 10^5$ kg, $I_{R0} = 4.8 \times 10^5$ kgm^2 and $I_{Rs} = I_{Rb} = 1.6 \times 10^5$ kgm^2, respectively. A rigid circular foundation with r=4 m on the ground surface is adopted to explore SSI (Mahmoud *et al.* 2012a, Takewaki 2005a, b). In order to perform parametric studies on the dynamic parameters of super structure, a vast range of the natural period of the superstructure has been studied in the range of $0.1s \leq T_s \leq 2s$. Furthermore, to evaluate the effects of soil-structure interaction, three types of soil, soft, medium and dense have been considered with the specifications given in Table 1.

Three types of soil, three well-known earthquakes and a vast range of period of the superstructure is considered. Simulation results indicate the necessity of considering SSI effects on the structures. In the second phase, these studies are carried out on a smart base-isolated structure.

The adopted control algorithm for tuning the control force has a key role in successful implementation of the structures; however, in most studied carried out in the literature, these algorithms are designed without considering the SSI effect. Earthquake loads are unpredictable stochastic loads. Therefore, if a controller is designed for a particular earthquake, there is no guarantee to be effective for other earthquakes. On the other hand, numerous time history analyses to achieve a reliable design of controller are time-consuming and costly. Conventionally, a spectral density function is used rather than a collection of time history input to tackle the problem. In stochastic analysis an artificial acceleration of the ground motion is simulated for modelling the possible earthquakes. It is produced by a band limited Gaussian white noise

Table 1 The parameters of soil and foundation (Liu *et al.* 2008)

Soil type	Poisson's ratio	Soil density (kg/m^3)	Shear-wave velocity (m/s)	Shear modulus (N/m^2)
Soft soil	0.49	1800	100	1.80×10^7
Medium soil	0.48	1900	300	1.71×10^8
Dense soil	0.33	2400	500	6.00×10^8

known as filter models (Mohebbi *et al.* 2013). Nagarajaiah and Narasimhan (2006) proposed a modified filter form the well-known Kanai-Tajimi filter. Considering a set of near-field and far-field earthquakes with different intensity and frequency content and applying the least squares fitting technique, they proposed the following power spectral density function to model an artificial earthquake in the area of the smart base-isolated building

$$s(\omega)=\frac{4\xi_g\omega_g\omega}{\omega^2+2\xi_g\omega_g\omega+\omega_g^2} \tag{16}$$

in which ξ_g and ω_g are the damping ratio and angular frequency of the ground, respectively. In the study, they considered as $\omega_g=2\pi$ *rad/sec* and ξ_g=0.3. The output of this filter simulates the earthquake which has been used for design of control system. It can be a suitable statistical representation of different earthquakes.

Linear-quadratic regulator (LQR) controller is one of the most commonly-used techniques to design of control system in seismic-excited structures. This technique can be used for both active and semi-active controls of buildings. In this controller, a cost function J is defined to determine the optimal control forces. In the area of the structural control, cost function is often associated with an acceptable level of structural response and control force. Hence, the cost function J in LQR controller is defined as follows (Fisco and Adeli 2011)

$$J=\int_0^{t_f}[\boldsymbol{Z}^T(t)\boldsymbol{Q}\boldsymbol{Z}(t)+\boldsymbol{f}^T(t)\boldsymbol{R}\boldsymbol{f}(t)]dt \tag{17}$$

where t_f is the duration of an earthquake. Also, the symmetric weighting matrices $\boldsymbol{Q}$ and $\boldsymbol{R}$ are the design parameters to obtain the required performance. Assuming the steady-state Riccati matrix and the corresponding steady-state Riccati equation, the control force vector in this method can be obtained by the following equation.

$$\boldsymbol{f}(t)=-\boldsymbol{G}\boldsymbol{Z}(t) \tag{18}$$

$\boldsymbol{G}$ is the control gain matrix which is obtained as

$$\boldsymbol{G}=\boldsymbol{R}^{-1}\boldsymbol{B}^T\boldsymbol{P} \tag{19}$$

where the steady-state Riccati matrix $\boldsymbol{P}$ is semi-positive definite matrix obtained from the following Riccati equation.

$$\boldsymbol{P}\boldsymbol{A}+\boldsymbol{A}^T\boldsymbol{P}-\boldsymbol{P}\boldsymbol{B}\boldsymbol{R}^{-1}\boldsymbol{B}^T\boldsymbol{P}+\boldsymbol{Q}=\boldsymbol{0} \tag{20}$$

Values of the members of the weighting matrices indicate the relative importance of state variables and control forces in the process of controller design. Allocating larger values to the members of the matrix $\boldsymbol{Q}$ indicates that reducing structural responses is the main objective and allocating larger amounts to members of the matrix R represents that the designer aims the use of less energy and power to apply the control forces. A good trade-off between two conflicting objectives can be achieved with by appropriate selecting the weighting matrices $\boldsymbol{Q}$ and $\boldsymbol{R}$ (Fisco and Adeli 2011). In this study, the weighting matrix $\boldsymbol{Q}$ is adopted as

$$\boldsymbol{Q}=\alpha\begin{bmatrix}\mathbf{I} & 0\\ 0 & 0.1\mathbf{I}\end{bmatrix} \tag{21}$$

It is notably that the floor displacement is about 0.1 of floors velocity. Therefore, corresponding to the structural responses in the term of the velocity vector, the coefficient of 0.1 is adopted. From a practical standpoint, the amount of control force is usually limited to 0.02W, in which W is the total weight of the structure. After a trial and error, it is found this limitation may be achieved by taking $R=10^{-5}$. Therefore, the problem of tuning the gain matrix **G** for the studied smart base-isolated is converted to the following optimization problem

$$\begin{cases} Find & \alpha \\ \text{minimize} & J \\ Subjected\ to & \max\|f(t)\|\le 0.02\ \text{W}\end{cases} \tag{22}$$

4. Results and discussion

The defined problem in Eq. (22) for tuning the gain matrix **G** forms an optimization problem. This problem includes many conflicting design objectives. Such optimization problems have many local optimums and require a heavy small-scale search. Also, it is not possible to define a continuous and explicit cost function for this problem. To cope with this, an evolutionary optimization algorithm keeping enough diversity of the population is required. The advantage of evolutionary algorithms compared to that of gradient-based algorithms is their "black box" character that makes only few assumptions about the underlying cost functions. Furthermore, the definition of cost functions usually requires lesser insight to the structure of the problem space than the manual construction of an admissible heuristic. They perform consistently well in many different problem categories. Also, they are able to handle complex optimization problems and take into account the nonlinearities of the problems (Weise 2009). PSO algorithm is a successful optimization algorithm which has been widely applied to the numerous engineering applications. It is inspired by social behavior of bird flocking or fish schooling. Easy to implement and having few parameters to adjust as well as s peed convergence are the important advantages of PSO rather than that some evolutionary optimization algorithm. PSO has been successfully applied in many optimization problems in engineering (Parsopoulos 2010, Du and Swamy 2016). Hence, the optimization problem defined in Eq. (22) is solved using PSO optimization algorithm to tune the gain matrix **G** of the smart base-isolated in both cases without and with considering SSI effects. The tuning of the gain matrix is carried out for the structure under the artificial earthquake excitation described in the previous section. Time-history analyses of the structure are carried out using

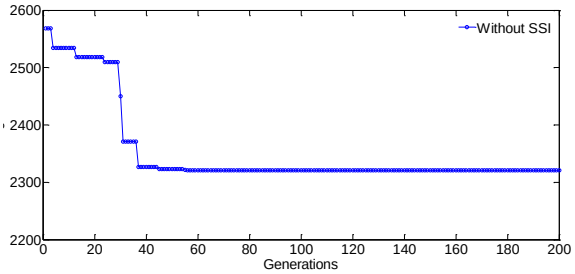

(a)

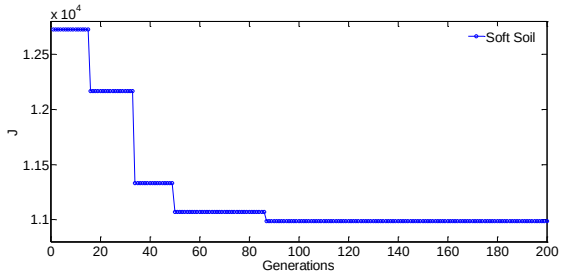

(b)

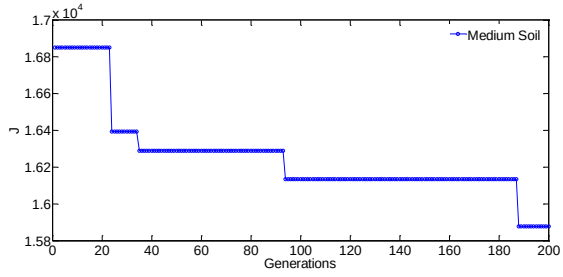

(c)

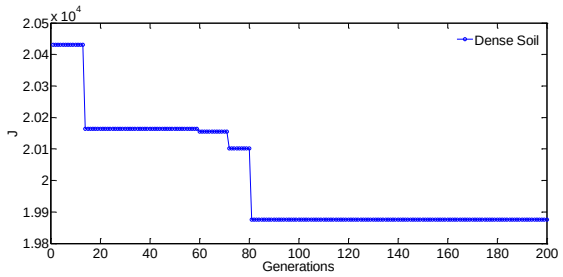

(d)

Fig. 2 The convergence histories of the PSO to minimize the cost function J

MATLAB/Simulink software (2000). The optimization process is done for a vast range of the natural period of the superstructure in the range of $0.1s \leq T_s \leq 2s$. The convergence histories of the PSO to minimize the cost function J are shown in Fig. 2 in the case of T_s = 1s for without SSI effects, soft, medium and dense soil. As can be seen from this figure that the convergence of the cost function has been achieved in 100 iterations for all cases; however, all of the operations is repeated up to about 200 iterations for obtaining the converged optimal solution.

Time histories of base displacement, top floor acceleration and the demanded control force of the both the base-isolated structure and smart base-isolated structure subjected to the artificial earthquake excitation in the case of T_s=1 s are shown in Figs. 3 to 5, respectively. These figures are representing in the cases of without SSI effects and three soil types. It is observed the base displacement of smart base-isolated structure is significantly decreased in comparison with the base-isolated structure. In the case of without SSI effects, the maximum base displacement of base-isolated structure is about 26.72 while this value is about 13.75 cm for the smart structure. It means that the adopted controller gives a reduction of 49% in comparison with the uncontrolled structure. Similarly, these reductions are resulted in about 61%, 61% and 62% in the cases of soft, medium and dense soils, respectively. The root-mean-square (RMS) of the base displacement as a reasonable index for assessment the control effectiveness is reduced about 49%, 52%, 53% and 53% in comparison with the uncontrolled structure in the cases of without SSI effects, soft, medium and dense soils, respectively. In comparison with uncontrolled structure, an increasing about 37% is observed in RMS superstructure acceleration of the smart isolated structure in the case of without SSI. In the cases of soft, medium and dense soils, the value of RMS superstructure acceleration reveals a reduction about 5%, 6% and 7%, respectively. Therefore, the controllers designed by PSO algorithm are able to provide a suitable performance in reducing the base displacements and their RMS. However, the results of the maximum and RMS floor accelerations indicate that any attempt to decrease the maximum base displacement may leads to increase the superstructure accelerations in comparison with the uncontrolled case. This result is reported in most researchers in the area of the smart base-isolated structures. In fact, the main goal of seismic control of base-isolated structures is to reduce the isolation displacement with accepting an increase in the superstructure acceleration. The time histories of the control forces are also shows that the maximum demanded control force of actuator in smart structure have not exceeded the typical practical values i.e., 0.02W.

In order to investigate the soil-structure interaction effects on seismic performance of smart base-isolated structures under different earthquake excitations, the artificial earthquake excitation was described in the previous section, El Centro (1940), Hachinohe (1968) and Kobe (1995) are considered. The peak ground acceleration (PGA) of the artificial earthquake excitation is scaled to 0.5 g. Also, the PGA of El Centro, Hachinohe and Kobe are 0.34 g, 0.22 g and 0.83 g, respectively.

To investigate the SSI effects on seismic performance of smart base-isolated structures with different natural periods, the numerical studied are also carried out on a vast range of the natural structural period in the cases of without SSI effects, soft soil, medium soil and dense soil.

Figs. 6 and 7 show the SSI effects on maximum and RMS base displacement responses for the smart base-isolated structure against natural periods of superstructure under different earthquakes, respectively. Similarly, the maximum and RMS top floor acceleration responses are illustrated in Figs. 8 and 9.

As can be seen, the maximum and RMS base displacements of the smart base-isolated structures considering SSI effects are more than the corresponding responses in the case of ignoring SSI effects. The seismic responses of structures are affected by the dynamical parameters of the structures and imposed earthquakes. The SSI effects significantly modify the dynamic characteristics of base isolated structures such as natural frequencies,

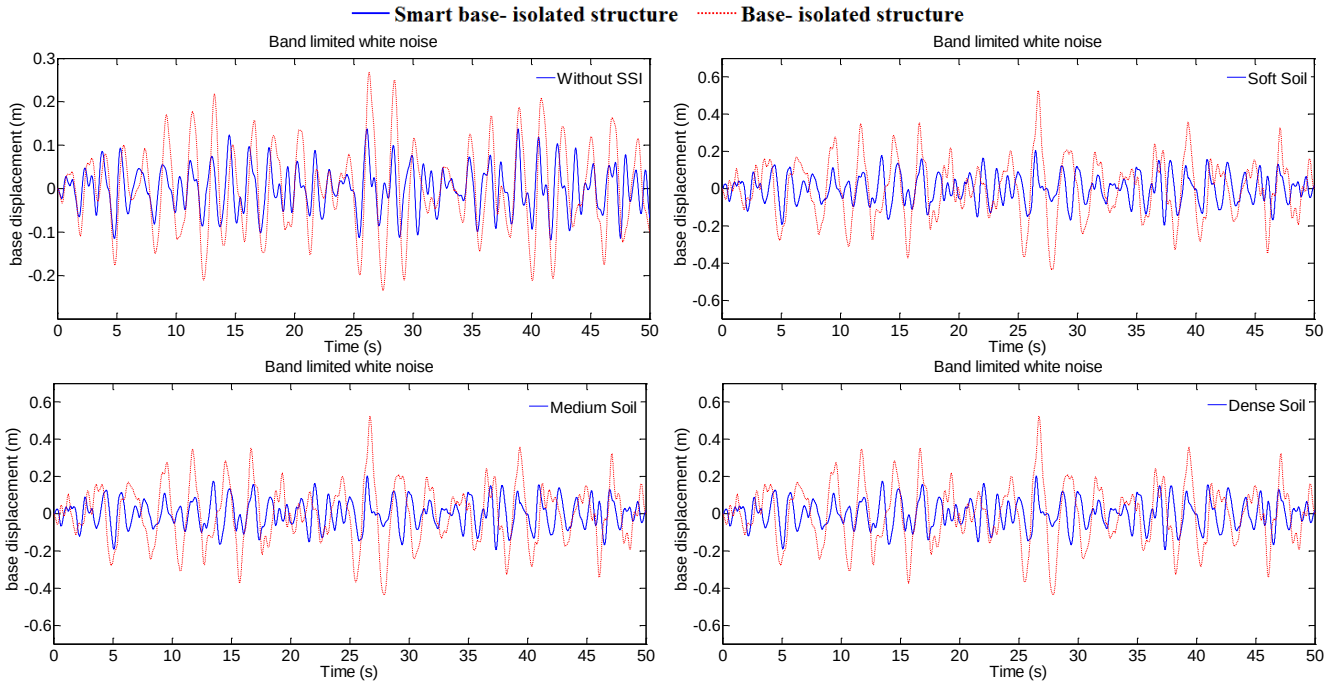

Fig. 3 Time histories of base displacement of the structure subjected to the artificial earthquake excitation in the case of T_s=1 s

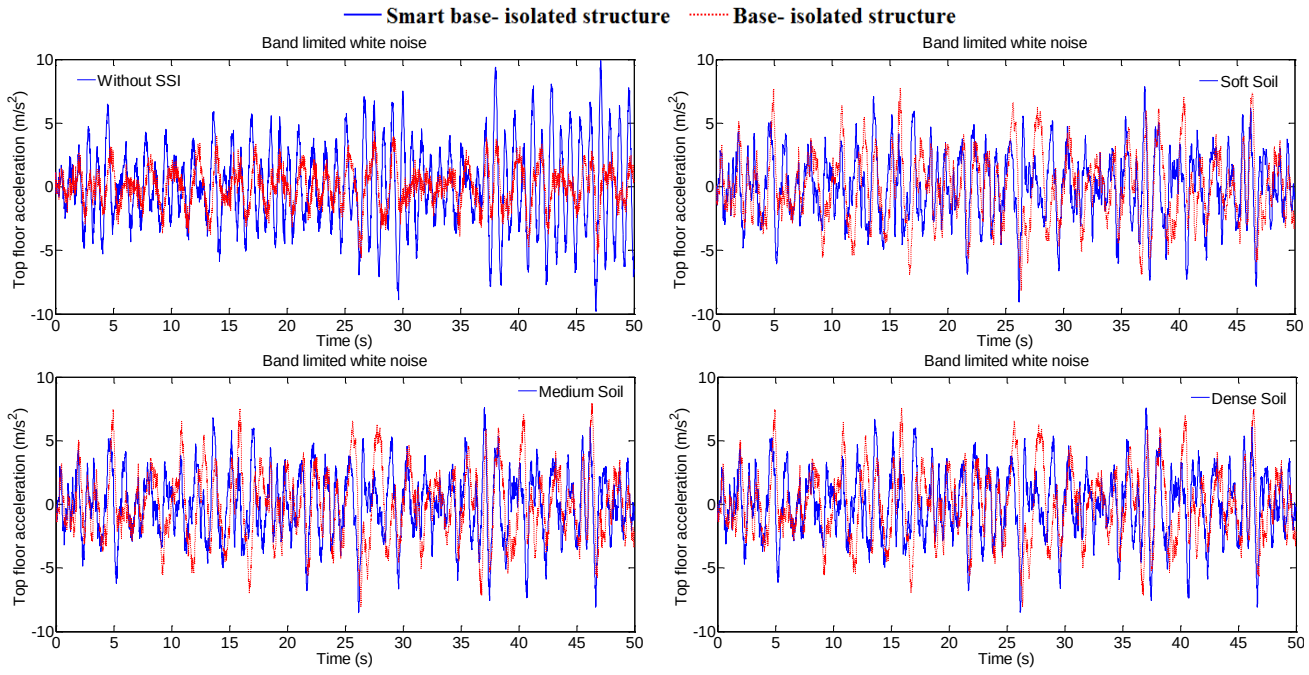

Fig. 4 Time histories of top floor acceleration of smart base-isolated structure subjected to the artificial earthquake excitation in the case of T_s=1 s

damping ratios and mode shapes. Based on the corresponding values of the spring stiffness and damping coefficients of the swaying and rocking effects, the structural dynamic parameters considering SSI effects may be very different from the case of without SSI effects. The natural frequency and damping ratio of the base isolated structure for the case of without SSI are obtained about 2.07 s and 0.09, while these parameters are about 2.56 s and 0.05 for the case of dense soil. On the other hands, based on the concept of structural control and closed loop control, the corresponding properties of the structure such as the natural frequency and damping ratio of the structure are modified for smart base isolated structure. The change rate depends on the feedback gain matrices designed for the smart structures which are different for the cases of without SSI and the dense soil. Consequently, the maximum response for the case of without SSI does not coincide with that of the dense soil.

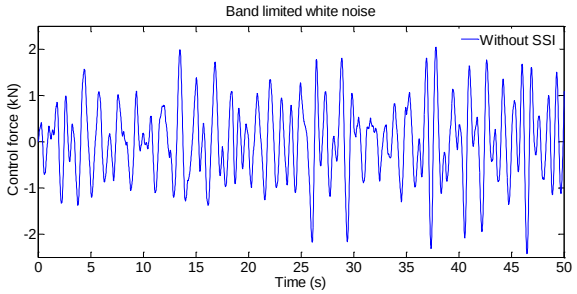

(a)

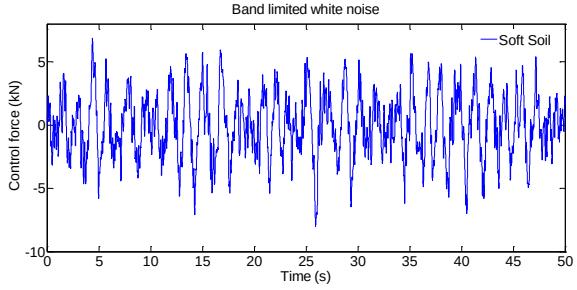

(b)

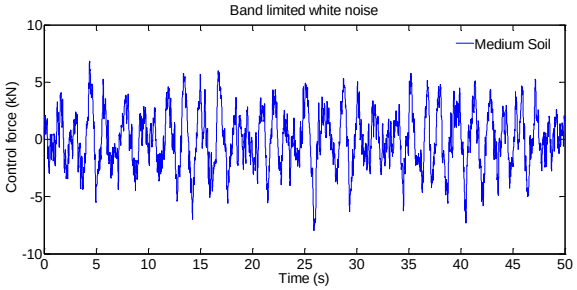

(c)

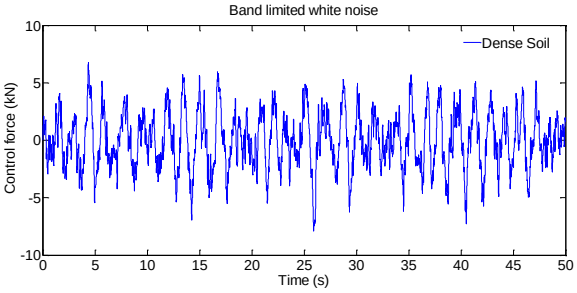

(d)

Fig. 5 Time histories of the demanded control force of smart base-isolated structure subjected to the artificial earthquake excitation in the case of T_s=1 s

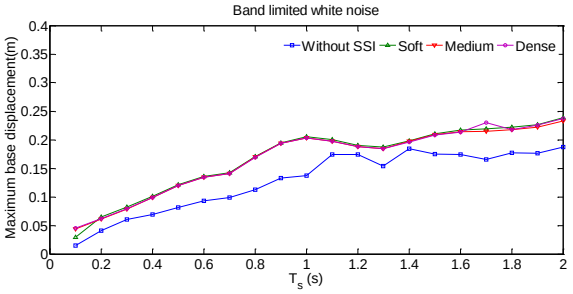

(a)

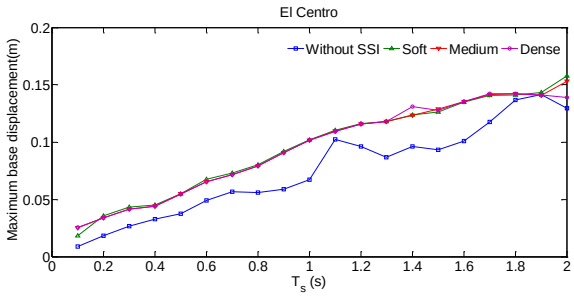

(b)

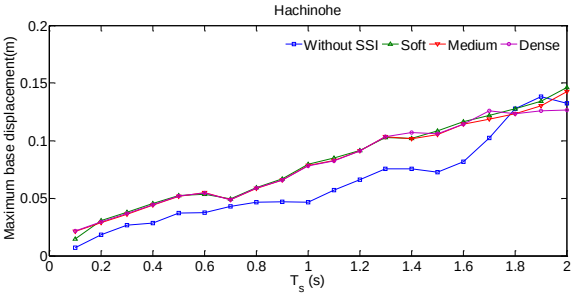

(c)

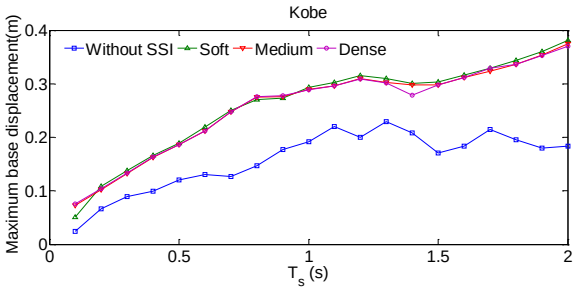

(d)

Fig. 6 The SSI effects on maximum base displacement responses for the smart base-isolated structure against natural periods of superstructure

In the case of SSI effects, the effect of soil type on modal properties and seismic responses is small, when the isolators are much more flexible, than the soil. The numerical studies in this paper are carried out on a benchmark base isolated structure introduced by Mahmoud *et al.* (2012a). Considering these parameters, the horizontal stiffness of isolator is 1.18 MN/m and the corresponding stiffness of the foundation are 381, 3600 and 11497 MN/m for soft, medium and dense soils. When the isolators are much more flexible than the soil, the soil type effects are limited on seismic responses of the base isolated structure. In other words, the contributions of the soils are much smaller than the isolators in the seismic responses of the base isolated structure. For earthquakes with a low PGA level, a slight increasing trend can be observed from the peak and RMS base displacement, while for earthquakes with a high PGA, a significant increasing is achieved. Overall, it is also observed that when the structural period increases, the maximum and RMS base displacement of structure increases as well, particularly for earthquakes with high PGA such as Kobe earthquake.

The SSI effects on maximum and RMS top floor acceleration responses for the smart base-isolated structure against natural periods of superstructure under different earthquakes are illustrated in Figs. 8 and 9. For the case of without SSI effects, the peak and RMS superstructure acceleration responses are different for the various ground

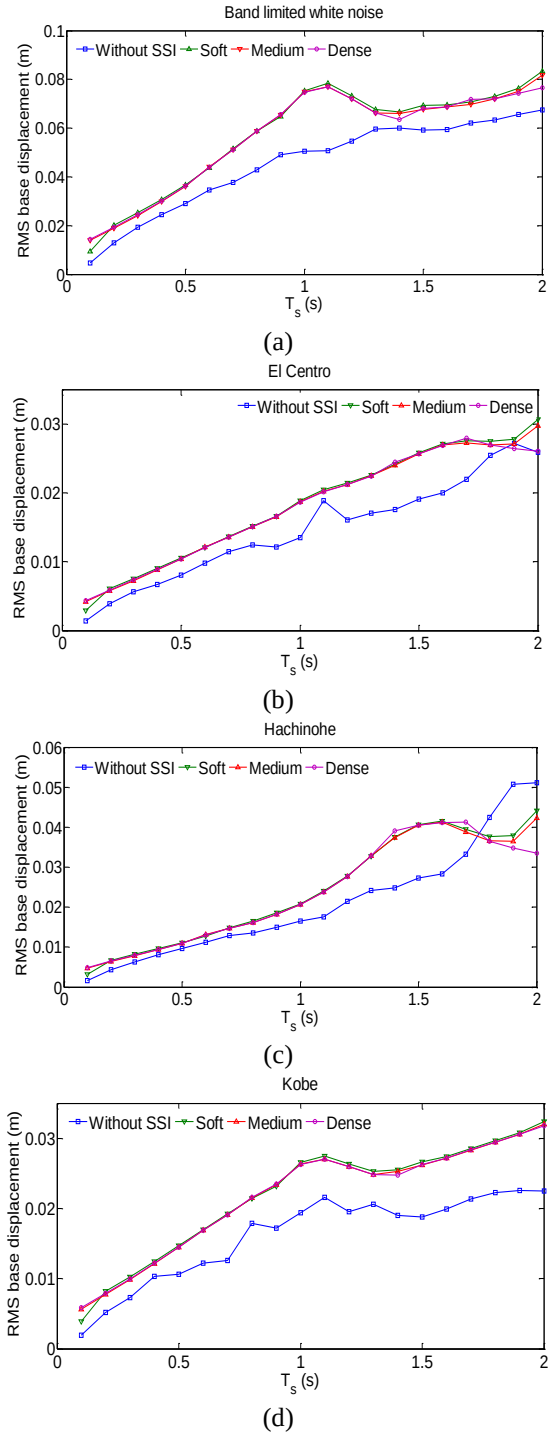

Fig. 7 The SSI effects on RMS base displacement responses for the smart base-isolate structure against natural periods of superstructure

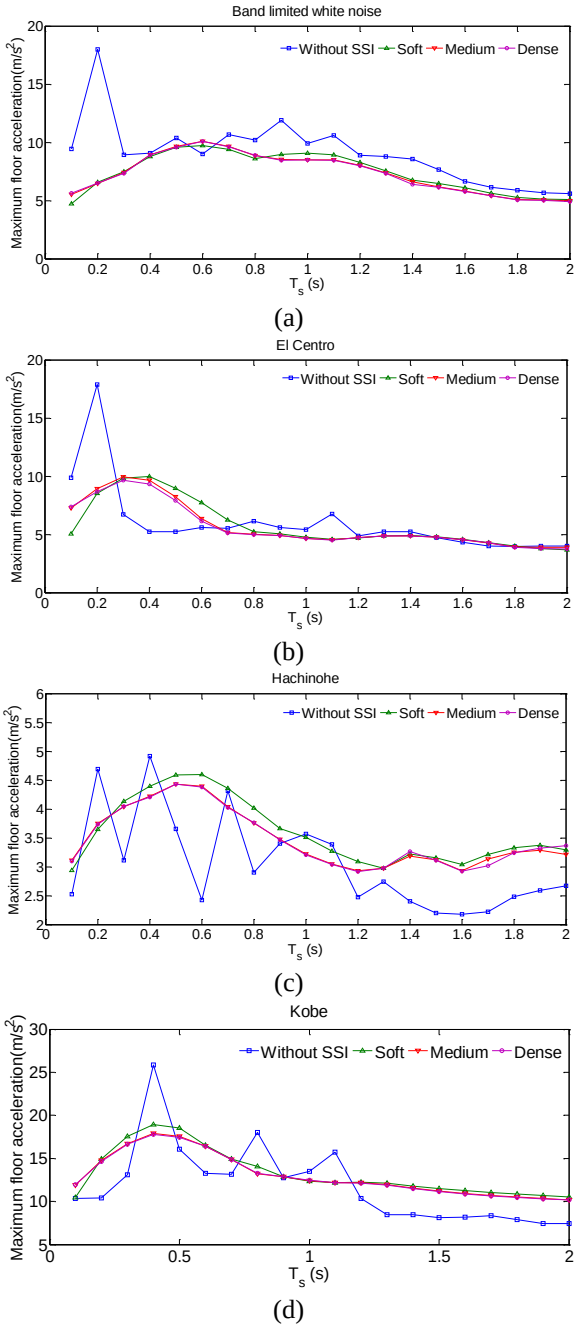

Fig. 8 The SSI effects on maximum top floor acceleration responses for the smart base-isolated structure against natural periods of superstructure

motions and natural periods. Considering El Centro earthquake, by increasing T_s up to about 0.2s, the maximum superstructure acceleration has been increased and then by increasing T_s, it has declined. Considering the RMS top floor acceleration responses for El Centro earthquake, it is not observed a certain order in the rate of changes of this response against natural periods of superstructures. Also, the results indicate that the maximum and RMS superstructure acceleration of the structure subjected to Kobe earthquake are occurred in T_s=0.4s. Overall, it can be concluded that the maximum and RMS superstructure acceleration of the smart base-isolated structure is significant influenced by the frequency content of earthquake excitations and the natural frequency of the superstructure. Considering the SSI effects for three type of soils, in low periods up to 0.5s (low-rise structures), the maximum top floor acceleration usually increases with increasing natural period of structures and then it experiences a slight reduction in the term of the maximum top floor acceleration.

As can be seen from Figs. 6 to 9, the seismic performance of smart base-isolated structures is very

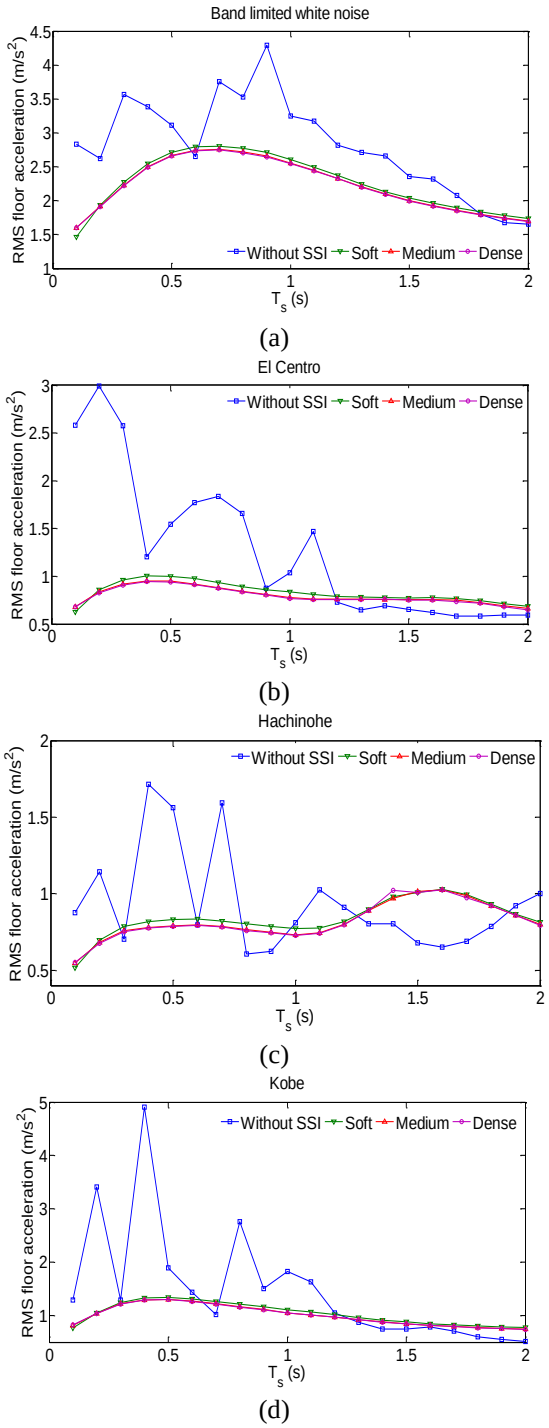

Fig. 9 The SSI effects on RMS top floor acceleration responses for the smart base-isolated structure against natural periods of superstructure

influenced by the SSI effect, so that ignoring them in the structural modelling will not reveal realistic and accurate results for the seismic behavior of the structures.

In order to evaluate the effect of considering SSI on the performance of controller, the designed controllers for the smart base-isolated structures without SSI effects are implemented on the models of smart base-isolated structures with SSI effects. For this purpose, two performance indices are, I_d and I_a, are defined as follows

$$I_d = \left(1 - \frac{max_t(u_b)}{max_t(\bar{u}_b)}\right) \times 100 \quad (23)$$

$$I_a = (1 - \frac{max_t(\ddot{u}_s)}{max_t(\ddot{\bar{u}}_s)}) \times 100 \quad (24)$$

where $max_t(u_b)$ represents the maximum base displacement of the exact structural model controlled by the designed controller with taking into account SSI effect. Also, $max_t(\bar{u}_b)$ indicates the corresponding response for the exact structural model controlled by the designed controller with ignoring SSI effects. The exact structural model is the smart base-isolated structure considering SSI effects. Similarly, the values of $max_t(\ddot{u}_s)$ and $max_t(\ddot{\bar{u}}_s)$ can be defined for the maximum top floor acceleration. Figs. 10-13 show these performance indices for the structures under artificial earthquakes, El Centro, Hachinohe and Kobe earthquakes and three types of soils. It is noteworthy that positive values indicate an increase and negative values indicate a decrease in response values. As one of the major issues in the design of controllers is the maximum control force requested by actuators, therefore, this value has been also given in the figures. In this figures, Case 1 represents the maximum demanded control force of the exact structural model controlled by the designed controller without SSI effects. Case 2 also represents the maximum demanded control force of the exact structural model controlled by the designed controller with SSI effects.

Considering the performance index I_d, the smart base-isolated experienced a significant increasing in term of maximum base displacement for all earthquakes and different frequencies. For example, in artificial earthquake excitation, an increase about 43% is resulted in the maximum base displacement for soft soil and T_s=0.3s. Similarly, this response increase about 47% and 46% for medium and dense soils, respectively. Considering El Centro earthquake, these raising points are about 61%, 69% and 68% for soft, medium and dense soils, respectively.

As previously mentioned, the superstructure acceleration response values are very influence on the natural period of the superstructure and frequency content of earthquake excitation. Investigation of performance index I_a shows that this amount has an increasing trend in some earthquakes and natural periods of superstructure. The increasing values are not significant, except in El Centro and Kobe. In fact, a reduction in the motion range of isolation system results in revealing a behavior close to that of the fixed base and consequently, acceleration of superstructure floors would enhance. But, it is notably that the main purpose of the intelligent design of base-isolated structures is reducing maximum base displacement for mitigating the structural damages. Increasing the acceleration of top floors often imposes non-structural damage to the structures. But, it should be noted that their values are often less than the corresponding values in the fixed-base structures. However, many attempts have recently carried out to propose effective control algorithms with the aim of overcoming this problem (Ozbulut and Hurlebaus 2010, Ozbulut *et al.* 2011, Zhao and Li 2015,

Zamani *et al.* 2017a, Zamani *et al.* 2017b).

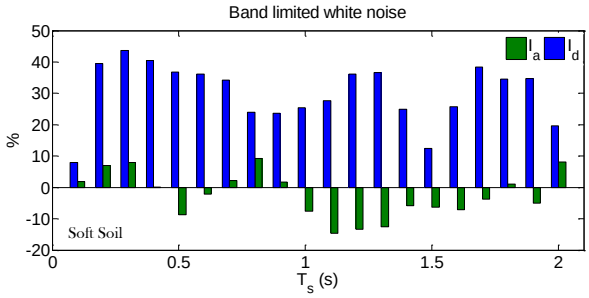

(a)

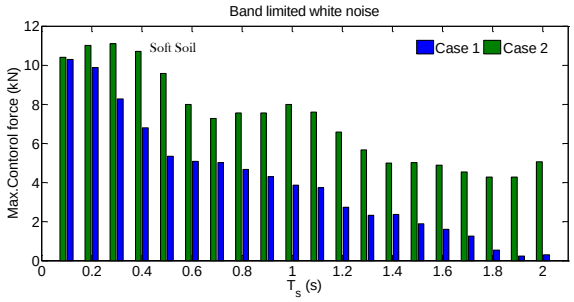

(b)

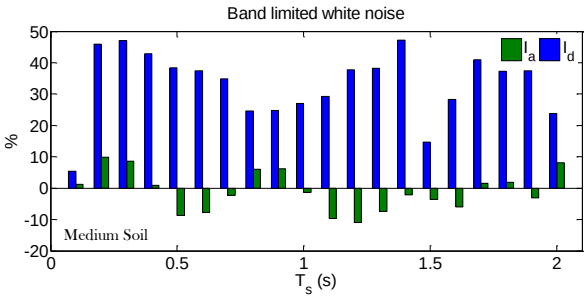

(c)

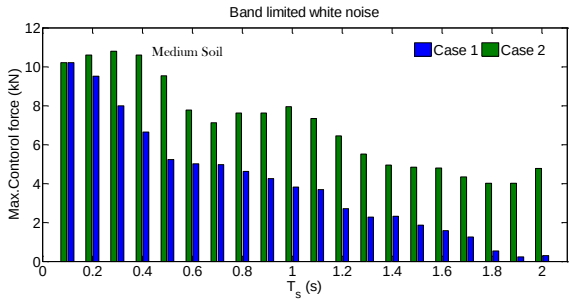

(d)

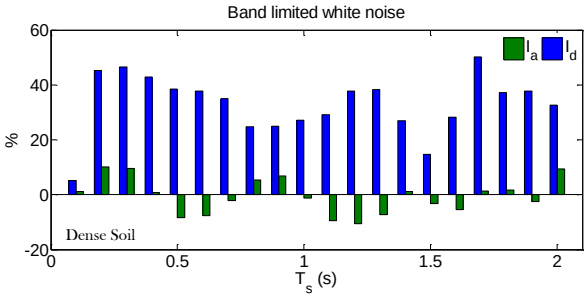

(e)

Fig. 10 Investigation considering the SSI effects on seismic performance of controller against natural periods of superstructure for artificial earthquakes

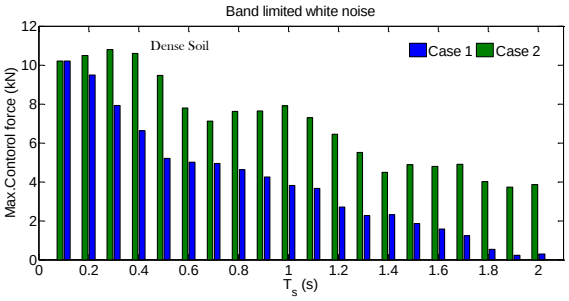

(f)

Fig. 10 Continued

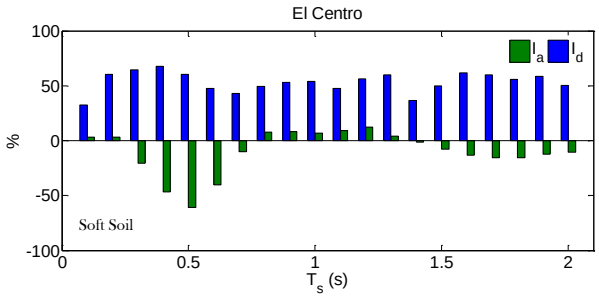

(a)

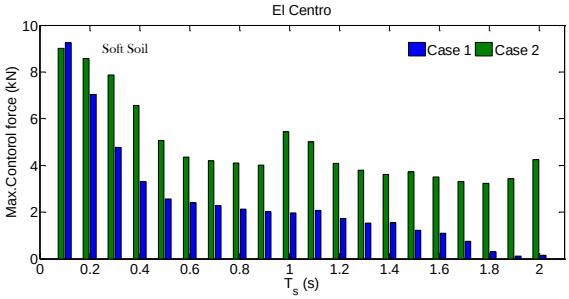

(b)

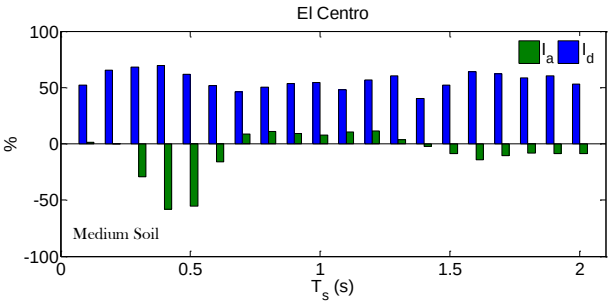

(c)

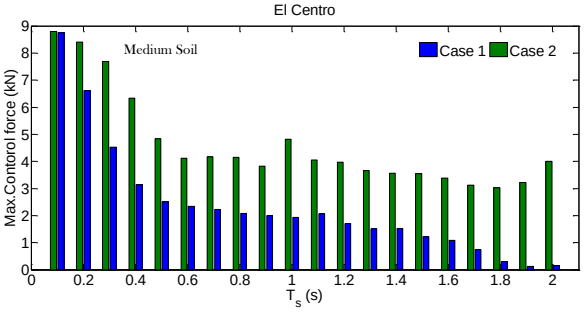

(d)

Fig. 11 Investigation considering the SSI effects on seismic performance of controller against natural periods of superstructure for El Centro earthquakes

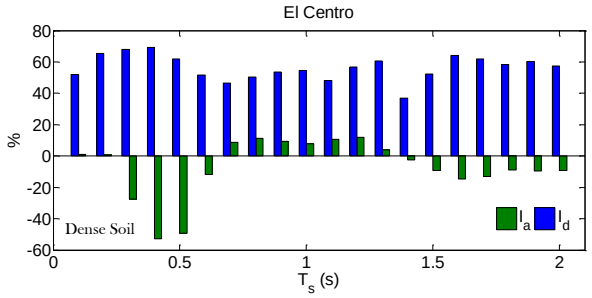

(e)

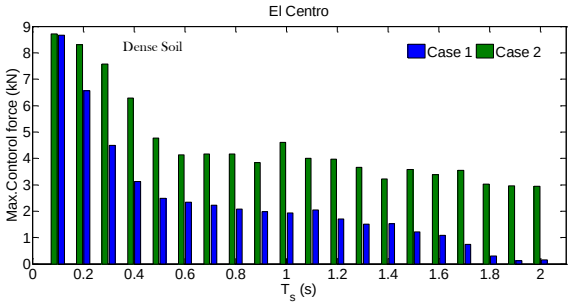

(f)

Fig. 11 Continued

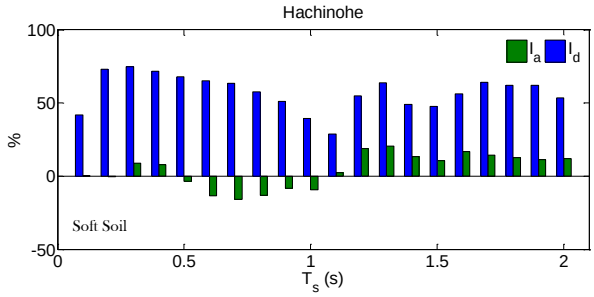

(a)

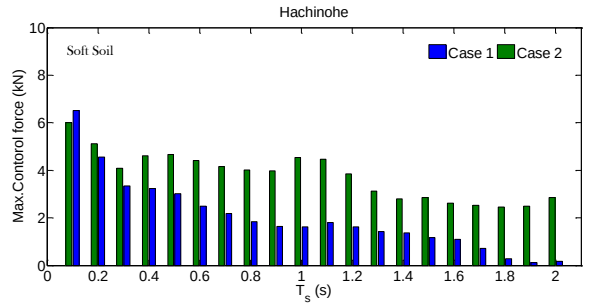

(b)

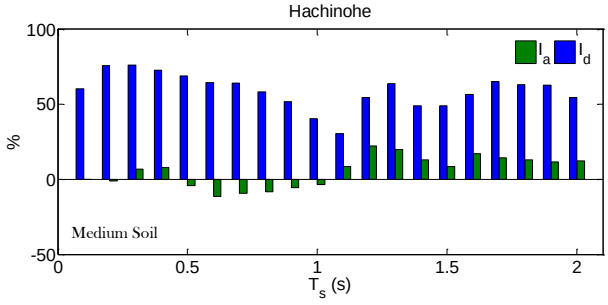

(c)

Fig. 12 Investigation considering the SSI effects on seismic performance of controller against natural periods of superstructure for Hachinohe earthquakes

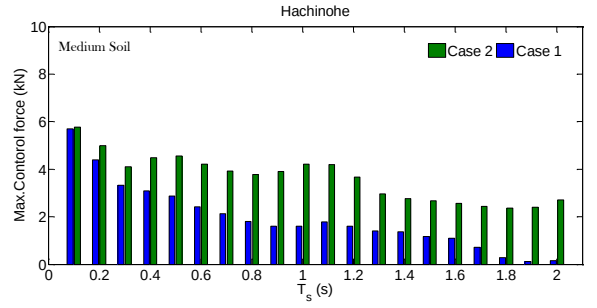

(d)

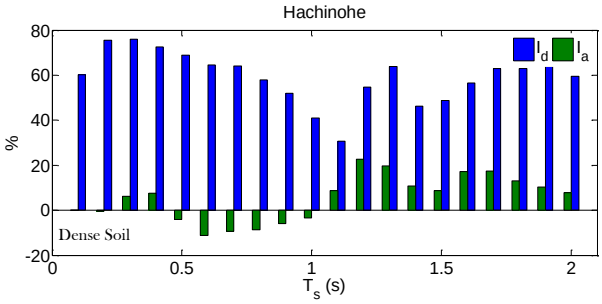

(e)

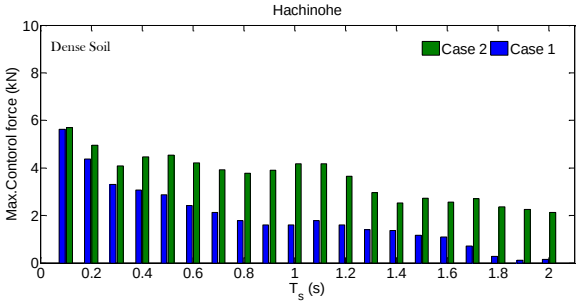

(f)

Fig. 12 Continued

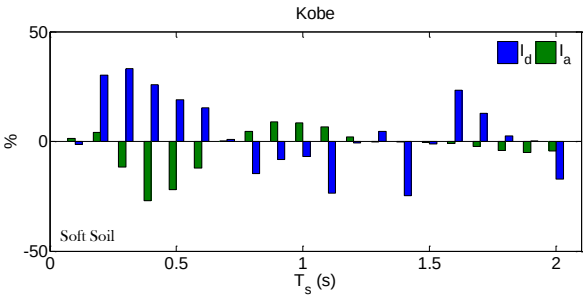

(a)

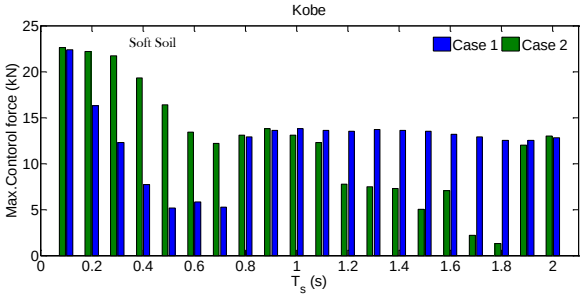

(b)

Fig. 13 Investigation considering the SSI effects on seismic performance of controller against natural periods of superstructure for Kobe earthquakes

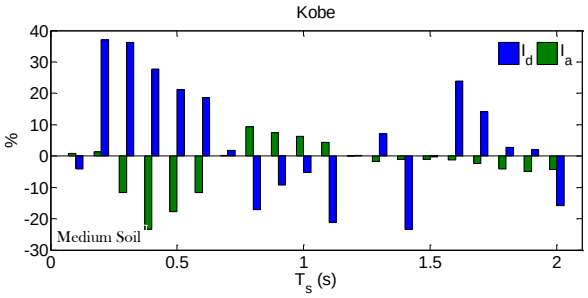

(c)

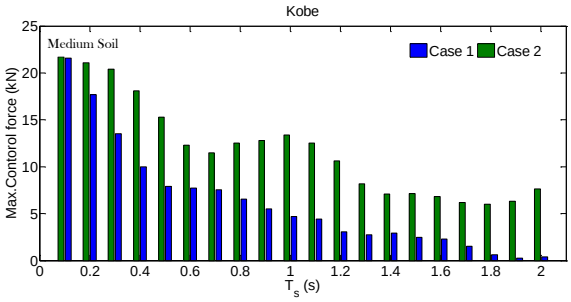

(d)

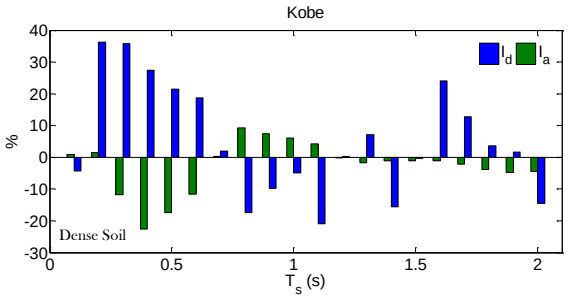

(e)

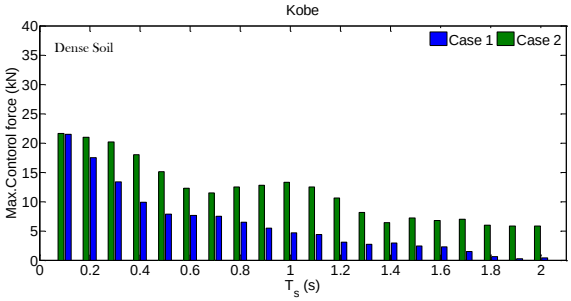

(f)

Fig. 13 Continued

As a general conclusion, it can be concluded that ignoring the SSI effects in the design process of a controller in smart base-isolated structure results in deterioration in the performance of controller in practical seismic applications.

Considering the maximum requested control forces illustrated in Figs. 10-13, it can be concluded the actuators often demanded larger control forces in the case where the controller is set considering the SSI effects in comparison with the case of ignoring SSI effect. With regard to the increasing base displacement in the cases of SSI effects, the actuator often demanded the higher control forces, whereas this issue is taken into account in design the control gain matrix of case 2, but this caution is not considered for Case 1. By increasing the period of superstructure, the structure demands less control forces from the actuators. In a small period range, there is no significant differences the maximum demanded control forces for three types of soils and two cases. It is notably that the period of the superstructure, the target period of isolation system, intensity and frequency content of an earthquake excitation and the control gain matrix designed for smart base isolated structure have key roles on seismic responses and the demanded control force of actuator. On the other hand, the control gain matrix modifies the dynamic parameters of the closed loop system of a smart isolated structure and effects on the value of the demanded control forces. Set of the mentioned conditions makes it difficult to achieve an overall conclusion about maximum control force and trend of its change. As can be seen, the maximum control force for Case 2 (with SSI) is higher than that for Case 1 (without SSI) in Figs. 11-13 except these conditions when the natural period of the superstructure on the soft soil is greater than 1.0 s under the Kobe earthquake in Fig. 13. Near-field earthquakes have long-duration pulses. They results in large displacements in the isolation system because the period of these pulses is coincides with the period of isolated structures. The control gain matrix of the smart base isolated structure for Case 1 (without SSI), subjected to Kobe earthquake as a near-field earthquake, was tuned in a way that demand more control force of the actuator. By increasing T_S and approaching the period of the structure to the period of pulses of near files earthquake excitations, the control gain matrix was tuned based on demanding larger control force. When this control gain matrix is implemented on the smart base isolated structure for Case 2 (soft SSI) demand large control force of actuator, while the period of the smart base isolated in Case 2 (soft SSI) and in large period (T_s>1) has significantly increased and it is far enough from the period of pulses of near files earthquake. These changes can be seen with much less intensity in other soils. Hence, the control gain matrix of case 2 that designed based on these conditions demand small control force of actuator, while the period change of structural system are not considered in the design of control gain matrix of case 1, so it demand greater control force. As a result it is found that the frequency content of earthquakes and its effect on the seismic responses of the smart base isolated structures plays an important role in the design controller.

5. Conclusions

In this paper, the effects of SSI on seismic performance of the smart base isolated structures were studied. While control algorithms commonly are designed for structures without considering the effects of SSI, a LQR controller is designed using PSO algorithm for seismic control of the smart base-isolated structures including SSI effects. Considering three types of soils, including soft, medium and dense soils and also three well-known earthquakes and an artificial earthquake, a vast range of numerical study was carried out on various natural periods of the superstructure in this study. A suitable performance of the adopted controller in reduction of the maximum and RMS base displacement was found. However, an increasing in the term of maximum and RMS superstructure acceleration may be resulted. Considering SSI effects, the maximum and RMS base displacements of the smart base-isolated

structures has been increased. In this case, the actuators demanded larger control forces. Overall, the maximum base displacement of the structure was increased by increasing the natural period of superstructure. It can also be concluded that the maximum and RMS top floor acceleration is significantly influenced by the frequency content of earthquake excitations and the natural frequency of the superstructure. By increasing the period of superstructure, the structure demanded less control forces from the actuators. The simulation results indicated that the design of the controller is very influenced by the SSI effects and frequency content of earthquakes. Furthermore, it is found that ignoring the SSI effect provides an unfavorable control system which may lead to a decline in the seismic performance of the smart-base isolated structure including the SSI effects.

References

Chaudhary, M.T.A., Abe, M. and Fujino, Y. (2001), "Identification of soil-structure interaction effect in base-isolated bridges from earthquake records", *Soil Dyn. Earthq. Eng.*, **21**(8), 713-725.

Cho, K.H., Kim, M.K., Lim, Y.M. and Cho, S.Y. (2004), "Seismic response of base-isolated liquid storage tanks considering fluid-structure-soil interaction in time domain", *Soil Dyn. Earthq. Eng.*, **24**(11), 839-852.

Constantinou, M.C. and Kneifati, M.C. (1986), "Effect of soil-structure interaction on damping and frequencies of base-isolated structures", *Proceedings of the 3rd U.S. National Conference on Earthquake Engineering*, Charleston, South Carolina, U.S.A., August.

Du, K.L. and Swamy, M.N.S. (2016), *Search and Optimization by Metaheuristics, Techniques and Algorithms Inspired by Mature*, Springer Int. Ltd., Switzerland.

Etedali, S. and Sohrabi, M.R. (2011), "Torsional strengthening of base-isolated asymmetric structures by increasing the flexible edge stiffness of isolation system", *J. Civ. Envrion. Eng.*, **11**(2), 51-59.

Etedali, S. and Sohrabi, M.R. (2016), "A proposed approach to mitigate the torsional amplifications of asymmetric base-isolated buildings during earthquakes", *KSCE J. Civ. Eng.*, **20**(2), 768-776.

Etedali, S., Sohrabi, M.R. and Tavakoli, S. (2013), "Optimal PD/PID control of smart base isolated buildings equipped with piezoelectric friction dampers", *Earthq. Eng. Eng. Vibr.*, **12**(1), 39-54.

Etedali, S., Tavakoli, S. and Sohrabi, M.R. (2016), "Design of a decoupled PID controller via MOCS for seismic control of smart structures", *Earthq. Struct.*, **10**(5), 1067-1087.

Fisco, N.R. and Adeli, H. (2011), "Smart structures: Part II-hybrid control systems and control strategies", *Scientia Iranica*, **18**(3), 285-295.

Iemura, H. and Pradono, M.H. (2002), "Passive and semi-active seismic response control of a cable-stayed bridge", *J. Struct. Contr. Health Monitor.*, **9**(3), 189-204.

Kim, M.K., Lim, Y.M., Cho, S.Y., Cho, K.H. and Lee, K.W. (2002), "Seismic analysis of base-isolated liquid storage tanks using the BE-FE-BE coupling technique", *Soil Dyn. Earthq. Eng.*, **22**(9), 1151-1158.

Kunde, M.C. and Jangid, R.S. (2006), "Effects of pier and deck flexibility on the seismic response of isolated bridges", *J. Bridge Eng.*, **11**(1), 109-121.

Liu, M.Y., Chiang, W.L., Hwang, J.H. and Chu, C.R. (2008), "Wind-induced vibration of high-rise building with tuned mass damper including soil-structure interaction", *J. Wind Eng. Ind. Aerodyn.*, **96**(6), 1092-1102.

Mahmoud, S., Austrell, P.E. and Jankowski, R. (2012a), "Simulation of the response of base-isolated buildings under earthquake excitations considering soil flexibility", *Earthq. Eng. Eng. Vibr.*, **11**(3), 359-374.

Mahmoud, S., Austrell, P.E. and Jankowski, R. (2012b), "Non-linear behaviour of base-isolated building supported on flexible soil under damaging earthquakes", *Key Eng. Mater.*, **488**, 142-145.

MATLAB (2000), *The Math Works*, Inc., Natick, Massachusetts, U.S.A.

Mohebbi, M., Shakeri, K., Ghanbarpour, Y. and Majzoub, H. (2013), "Designing optimal multiple tuned mass dampers using genetic algorithms (GAs) for mitigating the seismic response of structures", *J. Vibr. Contr.*, **19**(4), 605-625.

Nagarajaiah, S. and Narasimhan, S. (2006), "Smart base-isolated benchmark building. Part II: Phase I sample controllers for linear isolation systems", *Struct. Contr. Health Monitor.*, **13**(2-3), 589-604.

Ozbulut, O.E. and Hurlebaus, S. (2010), "Fuzzy control of piezoelectric friction dampers for seismic protection of smart base isolated buildings", *Bull. Earthq. Eng.* **8**(6), 1435-1455.

Ozbulut, O.E., Bitaraf, M. and Hurlebaus, S. (2011), "Adaptive control of base-isolated structures against near-field earthquakes using variable friction dampers", *Eng. Struct.*, **33**(12), 3143-3154.

Parsopoulos, K.E. (2010), *Particle Swarm Optimization and Intelligence: Advances and Applications: Advances and Applications*, IGI Global.

Perotti, F., Domaneschi, M. and De Grandis, S. (2013), "The numerical computation of seismic fragility of base-isolated nuclear power plants buildings", *Nucl. Eng. Des.*, **262**, 189-200.

Sarrazin, M., Moroni, O. and Roesset, J.M. (2005), "Evaluation of dynamic response characteristics of seismically isolated bridges in Chile", *Earthq. Eng. Struct. Dyn.*, **34**(4-5), 425-448.

Soneji, B.B. and Jangid, R.S. (2008), "Influence of soil-structure interaction on the response of seismically isolated cable-stayed bridge", *Soil Dyn. Earthq. Eng.*, **28**(4), 245-257.

Spyrakos, C.C. and Vlassis, A.G. (2002), "Effect of soil-structure interaction on seismically isolated bridges", *J. Earthq. Eng.*, **6**(3), 391-429.

Spyrakos, C.C., Koutromanos, I.A. and Maniatakis, C.A. (2009), "Seismic response of base-isolated buildings including soil-structure interaction", *Soil Dyn. Earthq. Eng.*, **29**(4), 658-668.

Spyrakos, C.C., Maniatakis, C.A. and Koutromanos, I.A. (2009), "Soil-structure interaction effects on base-isolated buildings founded on soil stratum", *Eng. Struct.*, **31**(3), 729-737.

Takewaki, I. (2005a), "Bound of earthquake input energy to soil–structure interaction systems", *Soil Dyn. Earthq. Eng.*, **25**(7), 741-752.

Takewaki, I. (2005b), "Frequency-domain analysis of earthquake input energy to structure-pile systems", *Eng. Struct.*, **27**(4), 549-563.

Tongaonkar, N.P. and Jangid, R.S. (2003), "Seismic response of isolated bridges with soil-structure interaction", *Soil Dyn. Earthq. Eng.*, **23**(4), 287-302.

Tsai, C.S., Chen, C.S. and Chen, B.J. (2004), "Effects of unbounded media on seismic responses of FPS-isolated structures", *Struct. Control Health Monitor.*, **11**(1), 1-20.

Vlassis, A.G. and Spyrakos, C.C. (2001), "Seismically isolated bridge piers on shallow soil stratum with soil-structure interaction", *Comput. Struct.*, **79**(32), 2847-2861.

Weise, T. (2009), *Global Optimization Algorithms-Theory and Application*.

Wolf, J.P. (1989), "Soil-structure-interaction analysis in time domain", *Nucl. Eng. Des.*, **111**(3), 381-393.

Zamani, A.A., Tavakoli, S. and Etedali, S. (2017a), "Control of

piezoelectric friction dampers in smart base-isolated structures using self-tuning and adaptive fuzzy proportional-derivative controllers", *J. Intell. Mater. Syst. Struct.*, **28**(10), 1287-1302.
Zamani, A.A., Tavakoli, S. and Etedali, S. (2017b), "Fractional order PID control design for semi-active control of smart base-isolated structures: A multi-objective cuckoo search approach", *ISA Trans.*, **67**, 222-232.
Zhao, D. and Li, Y. (2015), "Fuzzy control for seismic protection of semi active base-isolated structures subjected to near-fault earthquakes", *Math. Prob. Eng.*, (1), 1-17.